agriculture

MDPI

Article

Optimization of the Extraction Process for Anthocyanins from Tannat Grape Skins and Pomace and Research on Their Antioxidant and Anti-Aging Effects

Bing Wang [1], Yang Yu [1] and Honglei Wang [1,2,*]

[1] Yantai Institute of China Agricultural University, No. 2006, Bin Hai Zhong Road, Laishan District, Yantai 264670, China; 2023505520106@cau.edu.cn (B.W.); 2023505520127@cau.edu.cn (Y.Y.)
[2] Yantai Key Laboratory of Wine Flavour Technology, Yantai Institute of China Agricultural University, Yantai 264670, China
* Correspondence: wanghonglei@cau.edu.cn; Tel.: +86-13287988606

Abstract

Grape pomace is a major byproduct of winemaking and a rich source of bioactive anthocyanins with potential functional value. This study aimed to optimize anthocyanin extraction from Tannat grape pomace and evaluate its antioxidant and anti-aging activities. Ultrasonic-assisted extraction combined with a Box–Behnken design identified optimal conditions of 51.27 °C, 53.46% ethanol, 20.10 min ultrasonication, and a 1:24.05 solid-to-liquid ratio, yielding 186.21 ± 1.03 mg/100 g (R^2 = 0.9798, $p < 0.0001$). Tannat Grape Pomace Anthocyanins showed strong antioxidant capacity, with 2,2-Diphenyl-1-picrylhydrazyl scavenging of 89.44% ± 0.87% at 0.2 mg/mL (IC_{50} = 0.09 mg/mL) and 2,2′-Azino-bis (3-ethylbenzothiazoline-6-sulfonic acid) scavenging of 95.83% ± 0.54% at 0.75 mg/mL (IC_{50} = 0.26 mg/mL). In *Caenorhabditis elegans*, TGPA extended lifespan, improved motility, and increased heat and oxidative stress resistance without reducing reproductive capacity. Lifespan is a key indicator of aging. This study holds significant implications for advancing our understanding of the mechanisms underlying lifespan regulation, the connection between aging and disease, as well as the development of anti-aging therapies for humans. In conclusion, these findings indicate that Tannat Grape Pomace Anthocyanins possess promising antioxidant and anti-aging potential and support the sustainable, high-value utilization of grape pomace. This approach directly aligns with the core principles of sustainable agriculture by transforming an agricultural byproduct into a valuable resource.

Keywords: anthocyanin; antioxidant activity; *Caenorhabditis elegans*; anti-aging activity; response surface methodology; sustainable agriculture

Check for updates

Academic Editor: Vassilis Athanasiadis

Received: 2 December 2025
Revised: 2 January 2026
Accepted: 10 January 2026
Published: 16 January 2026

Copyright: © 2026 by the authors. Licensee MDPI, Basel, Switzerland. This article is an open access article distributed under the terms and conditions of the Creative Commons Attribution (CC BY) license.

1. Introduction

China's wine industry produces more than one million liters annually, generating large quantities of grape pomace as a byproduct. Currently, only a limited proportion of this material is used for purposes such as animal feed, fertilizer preparation, or biogas conversion, while most is discarded as waste [1]. This practice leads to environmental pollution and extensive resource loss. Addressing these challenges requires unlocking the biological value of grape pomace and developing efficient methods for its comprehensive utilization [2]. In this context, the valorization of grape pomace aligns with the principles of the circular economy, emphasizing the efficient use of resources and environmental protection through reduction, reuse, and recycling. Given the abundance of bioactive

compounds, particularly anthocyanins, in grape pomace, transforming it into value-added products could reduce environmental impact and provide novel raw materials for the food and pharmaceutical industries.

With socioeconomic development and rising living standards, consumer focus has shifted toward foods with nutritional and health-promoting attributes, making functional ingredients an important direction for future innovations in food science. Grape seeds and skins within pomace are rich in multiple high-value bioactive compounds. Among these, anthocyanins, representative water-soluble phytochemicals, have been well documented to possess antioxidant, anticancer, and anti-inflammatory properties, as well as regulatory effects on blood pressure and lipids, support for visual function, prevention of cardiovascular and cerebrovascular diseases, and delay of aging-related processes [3–10]. These characteristics align with the development goals of modern nutritional health foods and provide a promising entry point for the high-value transformation of grape pomace resources.

The Tannat grape, known for its rich polyphenolic content, is an ideal source of anthocyanins. Tannat grapes exhibit significantly higher levels of anthocyanins compared to other grape varieties, making them especially relevant for antioxidant and anti-aging research. This study aims to optimize the extraction process of anthocyanins from Tannat grape pomace, providing a foundation for large-scale industrial production. In the experiments, ultrasound-assisted extraction was selected due to its short extraction time, high efficiency, and simplicity [11,12]. Given the solubility and pH sensitivity of anthocyanins, ethanol, methanol, citric acid, and phosphoric acid were selected as extraction agents to identify the optimal conditions for large-scale applications [13]. The study also evaluates the antioxidant activity of the anthocyanin extract through in vitro assays to verify its biological potential, focusing on free radical scavenging capabilities. These findings lay the groundwork for further research into the anti-aging effects of the extract in vivo.

Aging refers to the progressive decline in an organism's physiological and psychological adaptability, ultimately leading to death [14]. It represents the combined result of multiple pathological, physiological, and psychological factors. Strategies to delay aging and extend lifespan have long been hot topics in scientific research [15]. The free radical theory is one of the classical hypotheses of aging, proposing that aging results from the progressive accumulation of free radicals produced by cellular metabolism. These free radicals can damage membrane structures, proteins, and DNA, accelerating the aging process [16]. *Caenorhabditis elegans* is widely recognized as an advantageous model organism for studying anti-aging and antioxidant mechanisms due to its high genetic homology with humans, short life cycle, transparent body, and suitability for large-scale laboratory cultivation. These characteristics make it an effective and reliable model for assessing the functional roles of bioactive compounds in dietary components [17,18].

This study investigates the antioxidant and anti-aging properties of anthocyanins extracted from wine grape pomace and optimizes their extraction process. The findings provide scientific support for evaluating their bioavailability and potential applications in health-oriented products, while offering theoretical guidance for industrial-scale utilization. By enhancing the value of grape pomace, this work contributes to improving the wine industry chain and promotes the sustainable, green development of local economies.

2. Materials and Methods

2.1. Materials and Chemicals

Tannat grape skins and pomace were obtained from Chateau State Guest (Danna grapes were harvested in September from grapevines planted in 2007 at the Chateau State Guest, Yantai, Shandong Province, China). The materials were dried at 40 °C, pulverized, and passed through a 100-mesh sieve. The resulting powder was vacuum-sealed in alu-

minum foil bags and stored at 4 °C in the dark until further use. Monohydrate citric acid, anhydrous methanol, anhydrous sodium acetate, anhydrous ethanol, and flake sodium hydroxide (China National Pharmaceutical Group Chemical Reagent Co., Ltd., Shanghai, China). Concentrated hydrochloric acid (Yantai Sanhe Chemical Reagent Co., Ltd., Yantai, China), analytical-grade phosphoric acid and potassium chloride (Shanghai Maclin Biochemical Technology Co., Ltd., Shanghai, China). LB broth, LB agar, and nematode growth medium (NGM) (Shandong Top Bioengineering Co., Ltd., Yantai, China). Total Antioxidant Capacity Assay Kit with ABTS method (Beijing Solare Technology Co., Ltd., Beijing, China).

2.2. Instrumentation

A PHS-3C pH meter (Shanghai Yidian Scientific Instrument Co., Ltd., Shanghai, China) and YP1002N electronic balance (China Shanghai Precision Scientific Instrument Co., Ltd. (Shanghai, China) were used. Absorbance was measured using a Thermo Fisher Scientific Evolution 300 UV-Vis spectrophotometer (Thermo Fisher Scientific Co., Ltd., Shanghai, China). Ultrasonic extraction was performed using KQ-300DE and KQ-3200DE digital ultrasonic cleaners (Kunshan Shumei Ultrasonic Instrument Co., Ltd., Kunshan, China). Centrifugation was carried out with an H2050R centrifuge (Hunan Xiangyi Laboratory Instrument Development Co., Ltd., Hunan, China). A BHS-4 digital constant-temperature water bath (Jiangyin Baoli Scientific Instrument Co., Ltd., Jiangyin, China) and a DHG-9053A forced-air drying oven (Shanghai Yiheng Scientific Instrument Co., Ltd., Shanghai, China) were also employed.

2.3. Optimal Extraction Solvent Screening

A total of 1.0000 g of Tannat grape pomace was placed into a conical flask, and the extraction solvent containing 3% phosphoric acid, 3% methanol, 3% citric acid, and 60% ethanol was added at a 1:25 solid-to-liquid ratio. The mixture was extracted at 50 °C for 20 min, followed by centrifugation at 4 °C and 8000 rpm for 10 min. The TGPA extraction yield in the supernatant was determined to identify the optimal extraction reagent.

2.4. Single-Factor Experiment

Five material-to-liquid ratios (1:15, 1:20, 1:25, 1:30, and 1:35 g/mL) and six extraction solvent concentrations (40.00%, 50.00%, 60.00%, 70.00%, 80.00%, and 90.00%) were set. Ultrasonic power levels were 100 W, 200 W, and 300 W. Extraction times were 10 min, 20 min, 30 min, 40 min, and 50 min. Extraction temperatures were 45 °C, 50 °C, 55 °C, 60 °C, and 65 °C. These five factors were systematically examined to evaluate their effects on TGPA extraction yield. Each condition was tested in triplicate.

2.5. Design of Response Surface Methodology (RSM)

Based on the single-factor experiments, a Box–Behnken response surface design was conducted using Design-Expert 13. Four independent variables, extraction temperature (A), solvent concentration (B), extraction time (C), and solid-to-liquid ratio (D), were selected, with TGPA extraction yield (Y) as the response variable. A four-factor, three-level optimization experiment was performed, as shown in Table 1.

Table 1. RSM Experimental Factors and Levels.

	A/°C	B/%	C/min	D
−1	45	40	10	1:20
0	50	50	20	1:25
1	55	60	30	1:30

2.6. Calculation of Anthocyanin Content

A 1.0 mL aliquot of extract was diluted to 10 mL using pH 1.0 and pH 4.5 buffers and equilibrated in the dark for 30 min. Absorbance was then measured at 520 nm and 700 nm. TGPA extraction yield was determined using the pH differential method:

$$\mathrm{A} = (\mathrm{A520} - \mathrm{A700})\mathrm{pH1.0} - (\mathrm{A520} - \mathrm{A700})\mathrm{pH4.5}$$

$$C(\mathrm{mg/100g}) = \frac{A \times 449.2 \times V}{26,900 \times m} \times DF \times 100$$

where A is the difference in absorbance between the two pH conditions (L/(g·cm)), C is the TGPA extraction yield in the sample (mg/100 g), V is the Total extract volume (mL), m is the mass of grape skin weighed (g), 26,900 is molar extinction coefficient of cyanidin-3-O-glucoside, (L/(mol·cm)), 449.2 is molecular mass of cyanidin-3-O-glucoside (g/mol), and DF is the Dilution factor.

2.7. In Vitro Evaluation of TGPA Antioxidant Capacity

2.7.1. Determination of DPPH Radical Scavenging Activity of TGPA

Following the procedure of ref. [19] with slight modifications, 0.0197 g of DPPH was accurately weighed and dissolved in anhydrous ethanol to a final volume of 50 mL. The solution was then diluted to obtain a 0.2 mmol/L DPPH working solution. A 100 µL aliquot of the 0.2 mmol/L DPPH ethanol solution was added to each well of a 96-well microplate, followed by 100 µL of the sample-containing ethanol solution. After thorough mixing, the microplate was incubated in the dark at room temperature for 30 min. Absorbance was measured at 517 nm using a microplate reader (Labselect 11510, 96-well tissue culture plate, Beijing Lanjieke Technology Co., Ltd., Beijing, China). The DPPH radical scavenging rate was calculated as follows:

$$\text{DPPH Radical Scavenging Rate } (\%) = (1 - \frac{A_S - A_{SB}}{A_C - A_{CB}}) \times 100$$

where AS represents the absorbance of the sample (100 µL sample solution + 100 µL DPPH radical solution); ASB represents the absorbance of the blank sample (100 µL sample solution + 100 µL anhydrous ethanol); AC represents the absorbance of sample C (100 µL anhydrous ethanol + 100 µL DPPH radical solution); and ACB denotes the absorbance of the blank control (200 µL of anhydrous ethanol).

2.7.2. Determination of ABTS Radical Scavenging Activity of TGPA

Freeze-dried TGPA extract was dissolved in 60% ethanol to prepare solutions at concentrations of 0.05, 0.1, 0.2, 0.3, 0.4, 0.5, 0.75, and 1 mg/mL. Antioxidant capacity was determined using the ABTS Radical Scavenging Assay Kit (Solaibao, Beijing, China). According to the kit instructions, samples were incubated in the dark at room temperature for 6 min, followed by absorbance measurement at 405 nm.

The ABTS radical scavenging rate was calculated using the following formulas:

$$\text{ABTS radical scavenging rate Dvc } (\%) = [(A_0 - A_{vc}) \div A_{control}] \times 100\%$$

$$\text{ABTS radical scavenging rate D}/\% = [A_0 - (A - A_{control})] \div A_{control} \times 100\%$$

2.8. TGPA Anti-Aging Activity Study

2.8.1. Preparation of *Escherichia coli* OP50 Culture

A single colony of *Escherichia coli* OP50 was streaked onto LB agar plates without antibiotics and incubated at 37 °C for 24 h. A single colony from the plate was then transferred into 100 mL of LB broth and incubated at 37 °C in a shaking incubator for 20 h.

2.8.2. Nematode Culture and Synchronization

Following the method of ref. [20] with minor modifications, nematodes and eggs were collected by washing NGM plates 1–2 times with M9 buffer in a laminar flow hood. The suspension was transferred to a 1.5 mL centrifuge tube and centrifuged at 3000 rpm for 1 min, after which the supernatant was discarded. A 1 mL aliquot of lysis buffer (5 M NaOH:5% NaClO:sterile water = 1:1:1) was added, and the tube was vortexed until nematodes lysed and the flocculent debris disappeared (not exceeding 5 min). The mixture was centrifuged at 3000 rpm for 1 min to pellet eggs, and the supernatant was discarded. The egg pellet was washed with 1 mL of M9 buffer, vortexed, and centrifuged at 3000 rpm for 1 min. This wash was repeated twice. The final egg pellet was resuspended in 1 mL M9 buffer and transferred onto NGM plates seeded with Escherichia coli OP50. Approximately 0.2 mL of the suspension was dispensed per plate, followed by incubation at 20 °C for 48 h to obtain synchronized L4-stage nematodes [21].

2.8.3. Experimental Groups

The blank control group consisted of NGM plates seeded with Escherichia coli OP50. Treatment groups were prepared by coating NGM plates with mixtures of TGPA extracts at various concentrations and OP50.

2.8.4. Nematode Lifespan Assay

Following the method of ref. [22] with minor modifications, synchronized adult nematodes were transferred onto four groups of NGM plates: blank control, 0.25 mg/mL, 0.5 mg/mL, and 0.75 mg/mL TGPA. Each group consisted of three plates, each with 30 nematodes, and was incubated at 20 °C. Day 0 represented the day of transfer. For the first 6 days, nematodes were transferred daily to fresh NGM plates containing the corresponding TGPA concentration. After day 6, transfers were performed every other day. Survival and mortality were recorded daily until all nematodes died.

Criteria for determining death were as follows: lack of movement when prodded with a nematode pick. “Abnormal” deaths were removed daily, including (1) nematodes dried on the plate walls, (2) nematodes accidentally killed during transfer, (3) nematodes lost due to burrowing into the agar. A survival curve was constructed using the recorded data.

2.8.5. Motor Activity Assessment

According to the method of ref. [23] with minor modifications, nematodes were exposed to 0.25 mg/mL, 0.5 mg/mL, and 0.75 mg/mL TGPA, along with a blank control. Each group included 30 nematodes, and the experiment was repeated three times. Motor activity was assessed on days 3, 6, and 9 of cultivation. Nematodes were categorized into three activity levels: Grade A, spontaneous movement without tactile stimulation; Grade B, movement only after gentle tactile stimulation; and Grade C, movement of only the head or tail after tactile stimulation. The numbers of nematodes in each grade were recorded, and the proportions were calculated.

2.8.6. Fertility Assay

L4-stage *Caenorhabditis elegans* (N2 strain) were grouped into batches of five nematodes per plate, with three plates per group, following the same grouping used in motility testing.

Adult nematodes were transferred daily to fresh plates at the same time each day for four consecutive days to allow egg laying during the peak reproductive period. All plates containing eggs were incubated at 20 °C. After approximately 2 days, when offspring reached the larval stage, the total number of progeny in each group was counted [24].

2.8.7. Nematode Heat Stress Experiment

Using the same culture method as in the lifespan assay, synchronized L4-stage nematodes were treated with TGPA extracts at 1 mg/mL, 2 mg/mL, and 3 mg/mL for 3 days, along with a blank control group. Each group consisted of three plates, each with 20 nematodes. After treatment, the incubator temperature was increased to 37 °C, designated as 0 h. Nematode survival was recorded hourly until all nematodes died [25,26].

2.8.8. Acute Oxidative Stress Experiment

For the oxidative stress assay, synchronized L4-stage nematodes were cultured as described above and treated with TGPA for 3 days, using the same concentration groups as in the heat stress experiment. Each group consisted of three parallel plates with 20 worms per plate. Nematodes were then transferred onto NGM plates containing 1.5% hydrogen peroxide (prepared in sterile M9 buffer). Survival was assessed every 30 min, and survival rates were calculated until all nematodes died.

2.9. Data Processing

Significant differences were analyzed using SPSS 27.0.1 (IBM Corp., Armonk, NY, USA), with $p < 0.05$ considered statistically significant. Data visualization was performed using OriginPro 2024b (OriginLab Corporation, Northampton, MA, USA) and GraphPad Prism 9.5 (GraphPad Software, LLC, San Diego, CA, USA). All experiments were conducted in triplicate.

3. Results

3.1. Optimization of TGPA Extraction Process

3.1.1. Screening for Optimal Extraction Reagent

As shown in Figure 1, TGPA extraction yields obtained with the four tested reagents ranged from 12.11 ± 4.63 mg/100 g to 152.79 ± 3.93 mg/100 g. Among all solvents, 60% ethanol produced the highest yield, while 3% methanol resulted in the lowest. The extraction efficiency achieved with 60% ethanol was significantly higher than that of the other reagents, and the safety profile of ethanol aligns with the requirements of both the food and pharmaceutical industries, indicating that 60% ethanol is the most suitable solvent for TGPA extraction.

3.1.2. Effect of Different Solid-to-Liquid Ratios on TGPA Extraction Yield

TGPA extraction yields under different solid-to-liquid ratios ranged from 106.71 ± 3.57 mg/100 g to 154.46 ± 2.69 mg/100 g. As shown in Figure 1, the extraction yield initially increased with increasing solvent volume, then declined. The yield at a 1:25 ratio was significantly higher than that of the other groups, demonstrating that this ratio is optimal. The subsequent decline in extraction efficiency may be due to the excessive solvent volume, which increases the likelihood of co-extraction of impurities. Polysaccharides and proteins can form stable complexes with anthocyanins via hydrogen bonding and hydrophobic interactions. These complexes alter the absorbance characteristics of anthocyanins, preventing their accurate inclusion in the calculation of the "effective anthocyanin content" and lowering the reported extraction yield. This observation is consistent with the impurity

interference phenomenon reported by ref. [27] in their study on anthocyanin extraction from blueberry pomace.

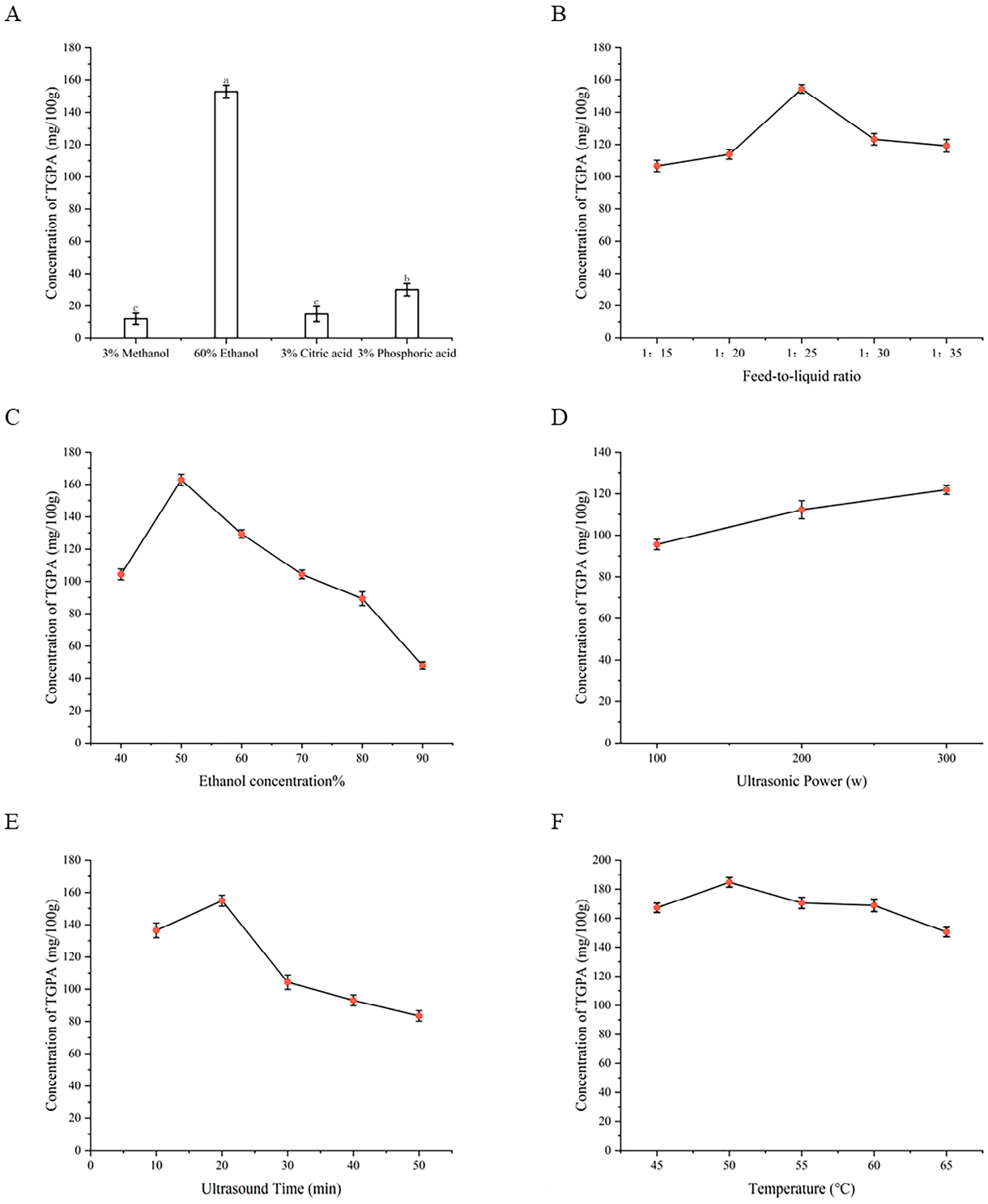


Figure 1. Single-factor test for the extraction of TGPA (**A**–**F**). In (**A**), different lowercase letters (a–c) above the bars indicate statistically significant differences among groups ($p < 0.05$).

3.1.3. Effect of Different Concentrations on TGPA Extraction Yield

As shown in Figure 1, ethanol concentrations between 40.00% and 90.00% produced TGPA extraction yields ranging from 48.01 ± 2.44 mg/100 g to 162.81 ± 3.43 mg/100 g. The extraction trend followed an initial decline, a subsequent increase, and a final decrease. The

maximum yield was observed at an ethanol concentration of 50.00%. At this concentration, the polarity of the mixed solvent closely matched that of grape anthocyanins, promoting efficient anthocyanin dissolution and yielding the highest extraction rate. Beyond 50.00%, increasing ethanol concentration reduced solution polarity, decreased compatibility with the strongly polar anthocyanins, and decreased their solubility. This significantly decreases anthocyanin solubility in high-concentration ethanol, reducing the amount that can reach saturation and ultimately lowering extraction efficiency. Moreover, high ethanol concentrations increase the solubility of non-polar or weakly polar substances, further reducing extraction efficiency. Therefore, 50.00% ethanol was identified as the optimal solvent concentration.

3.1.4. Effect of Ultrasonic Power on TGPA Extraction Yield

At an ultrasonic power of 300 W, TGPA extraction reached 121.90 ± 2.24 mg/100 g, representing the highest yield among the tested power levels. Extraction at 100 W and 200 W produced yields of 95.60 ± 2.49 mg/100 g and 112.30 ± 4.35 mg/100 g, corresponding to reductions of 21.58% and 7.88% relative to 300 W. Thus, 300 W was determined to be the optimal ultrasonic power.

3.1.5. Effect of Ultrasonication Time on TGPA Extraction Yield

As shown in Figure 1, TGPA yields under different ultrasonication times ranged from 83.49 ± 3.26 mg/100 g to 154.88 ± 3.44 mg/100 g. Extraction increased progressively as ultrasonication time increased, showing increased dissolution of anthocyanins through extended solvent–material contact. The highest yield was achieved at 20 min. However, beyond 20 min, the extraction efficiency decreased significantly. Prolonged ultrasonication may lead to structural degradation of previously extracted anthocyanins due to excessive cavitation or localized heating, reducing the measurable anthocyanin content. Therefore, 20 min was identified as the optimal ultrasonication time.

3.1.6. Effect of Ultrasonic Temperature on TGPA Extraction Yield

As shown in Figure 1, the TGPA extraction yield initially increased with increasing ultrasonic temperature and then declined. At 50 °C, the extraction yield was significantly higher than that of the other groups. An increase in temperature enhances solvent penetration, anthocyanin solubility, and the diffusion coefficient of solutes, improving mass transfer efficiency and promoting anthocyanin release into the extraction medium. However, at excessively high temperatures, heat-sensitive polyphenols and anthocyanins may undergo thermal degradation, leading to reduced stability and lower measurable levels. Thus, based on the single-factor results, ultrasonication at approximately 50 °C provided the most stable extraction conditions, with the highest TGPA content observed at 50 °C.

3.1.7. Response Surface Optimization of the Extraction Process

To further optimize extraction conditions, four variables, extraction temperature, solvent concentration, extraction time, and solid-to-liquid ratio, were selected for Box–Behnken RSM analysis, using TGPA yield as the response variable. The design and the experimental results are presented in Tables 2 and 3, respectively.

Table 2. Response RSM Design and Results for TGPA Extraction Process.

Test Number	A/Extraction Temperature/°C	B/Extraction Concentration (%)	C/Extraction Time (min)	D/Extraction Ratio (g/mL)	Concentration of TGPA (mg/100 g)
1	55	50	20	30	149.605
2	45	50	20	30	149.305
3	55	40	20	25	142.04
4	45	50	20	20	165.319
5	50	50	20	25	192.455
6	50	60	20	30	143.95
7	50	50	30	20	167.332
8	55	60	20	25	141.698
9	45	40	20	25	132.912
10	50	50	10	20	169.327
11	50	40	20	20	143.269
12	50	50	20	25	193.212
13	50	50	20	25	195.125
14	50	40	30	25	137.096
15	50	50	20	25	191.212
16	50	40	10	25	140.183
17	55	50	20	20	153.296
18	50	40	20	30	147.261
19	45	50	10	25	153.183
20	50	50	30	30	151.964
21	50	50	20	25	190.125
22	50	50	10	30	157.3
23	45	60	20	25	153.465
24	50	60	30	25	138.183
25	50	60	20	20	175.321
26	45	50	30	25	131.329
27	50	60	10	25	167.154
28	55	50	30	25	141.941
29	55	50	10	25	142.339

Table 3. Analysis of Variance for RSM Regression Model.

Source	Sum of Squares	df	Mean Square	F-Value	*p*-Value	Significance
Model	10,641.58	14	760.11	48.39	<0.0001	**
A—Extraction Temperature	17.756	1	17.75	1.13	0.3058	
B—Extraction concentration	494.22	1	494.22	31.46	<0.0001	**
C—Extraction Time	316.63	1	316.63	20.16	0.0005	**
D—Extraction Ratio	462.25	1	462.25	29.43	<0.0001	**
AB	109.15	1	109.15	6.95	0.0196	*
AC	115.08	1	115.08	7.33	0.0170	*
AD	37.97	1	37.97	2.42	0.1423	
BC	167.49	1	167.49	10.66	0.0056	**
BD	312.64	1	312.64	19.90	0.0005	**
CD	2.79	1	2.79	0.18	0.6798	
A^2	4534.90	1	4534.90	288.68	<0.0001	**
B^2	4277.08	1	4277.08	272.27	<0.0001	**
C^2	2950.78	1	2950.78	187.84	<0.0001	**
D^2	909.15	1	909.15	57.88	<0.0001	**
Residual	219.92	14	15.71			
Lack of Fit	205.25	10	20.53	5.60	0.0557	
Pure Error	14.67	4	3.67			
Cor Total	10,861.51	28				
$R^2 = 0.9798$						

Note: * indicates significant difference, $p < 0.05$; ** indicates highly significant difference, $p < 0.01$.

Using Design-Expert 13 to analyze the RSM data, the quadratic multiple regression equation describing the relationship between anthocyanin content (Y) and the four inde-

pendent variables, temperature (A), solvent concentration (B), extraction time (C), and solid-to-liquid ratio (D), was obtained as follows:

$$Y = -3747.5009 + 105.5184 \times A + 37.2585 \times B + 6.3070 \times C + 25.4498 \times D - 0.1045 \times A \times B + 0.1073 \times A \times C + 0.1232 \times A \times D - 0.0647 \times B \times C - 0.1768 \times B \times D - 0.0167 \times C \times D - 1.0576 \times A2 - 0.2568 \times B2 - 0.2133 \times C2 - 0.4736 \times D2 \quad (1)$$

As shown in Table 3, the regression model was highly significant ($p < 0.0001$), and the coefficient of determination ($R^2 = 0.9798$) indicated excellent model fit. An R^2 value this close to 1 demonstrates that the model reliably predicts TGPA extraction yield and is suitable for optimization analysis. The relative influence of each extraction factor followed the order: B > D > C > A, indicating that solvent concentration (B), solid-to-liquid ratio (D), extraction time (C), and extraction temperature (A) had descending influence on TGPA extraction yield. In response surface plots, steeper slopes and denser contour lines indicated stronger interaction between two factors, often forming an elliptical contour. On the other hand, flatter surfaces or circular contours indicated weaker interactions. As illustrated in Figure 2, significant interaction effects were observed between: temperature (A) and solvent concentration (B), temperature (A) and extraction time (C), temperature (A) and solid-to-liquid ratio (D), concentration (B) and time (C), concentration (B) and solid-to-liquid ratio (D), and time (C) and solid-to-liquid ratio (D). These interactions shaped the final extraction efficiency.

Based on model optimization, the ideal extraction conditions were determined as follows: extraction temperature: 51.27 °C; ethanol concentration: 53.46%; ultrasonication time: 20.10 min; solid-to-liquid ratio: 1:24.05. Under these optimized parameters, the theoretical TGPA yield was 190.24 mg/100 g. Verification experiments performed three times under the same conditions yielded 186.21 ± 1.03 mg/100 g, demonstrating excellent agreement with the predicted value and confirming the reliability of the regression model.

Compared with traditional extraction methods, the ultrasound-assisted extraction process optimized in this study offers advantages such as high extraction efficiency, short processing time, and reasonable solvent consumption. It is comparable to the efficiency of the two-step biocatalytic extraction of anthocyanins from red grape pomace reported by ref. [28] while being simpler in operation, lower in cost, and more suitable for industrial-scale application.

3.2. In Vitro Antioxidant Studies of TGPA

3.2.1. DPPH Radical Scavenging Activity

The DPPH radical scavenging activity of TGPA is presented in Figure 3. Within the tested mass concentration range, TGPA exhibited a clear dose-dependent increase in antioxidant activity. As TGPA concentration increased, the radical scavenging rate increased correspondingly. At a TGPA concentration of 0.2 mg/mL, the scavenging rate was 89.44% ± 0.87%, with an IC_{50} of 0.09 mg/mL. These findings indicate that TGPA possesses strong hydrogen-donating ability and effectively neutralizes DPPH free radicals.

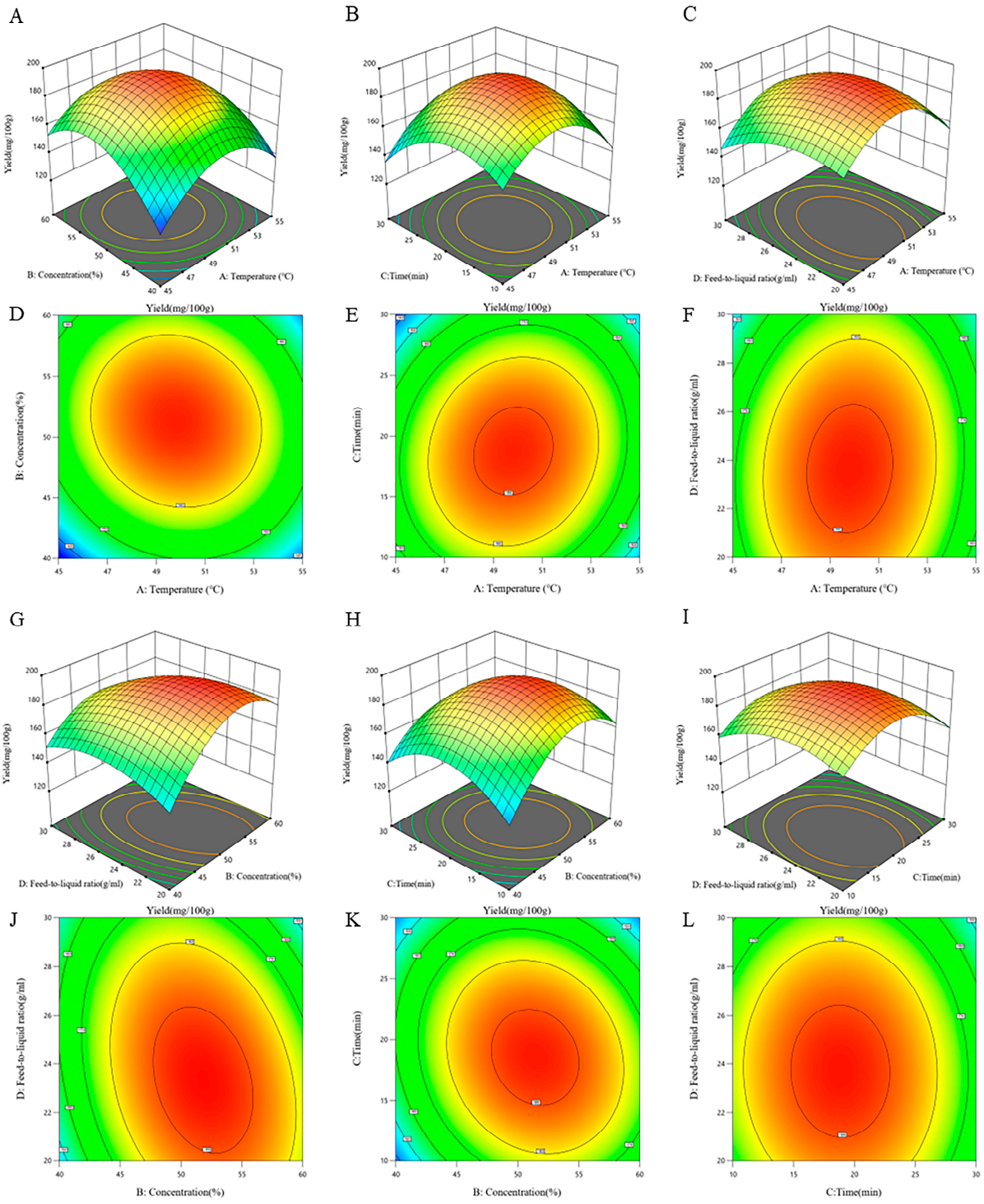


Figure 2. Response Surface Diagram and Contour Plots of the Effect of Factor Interactions on TGPA Extraction Yield (**A**–**L**).

3.2.2. ABTS Radical Scavenging Capacity

TGPA also demonstrated significant ABTS radical scavenging activity. As shown in Figure 3, the scavenging rate increased progressively with increasing TGPA concentration. At 0.75 mg/mL, TGPA achieved a scavenging rate of 95.83% ± 0.54% and an IC_{50} value of 0.26 mg/mL. The strong ABTS radical-quenching activity further supports the potential of TGPA as a potent antioxidant ingredient.

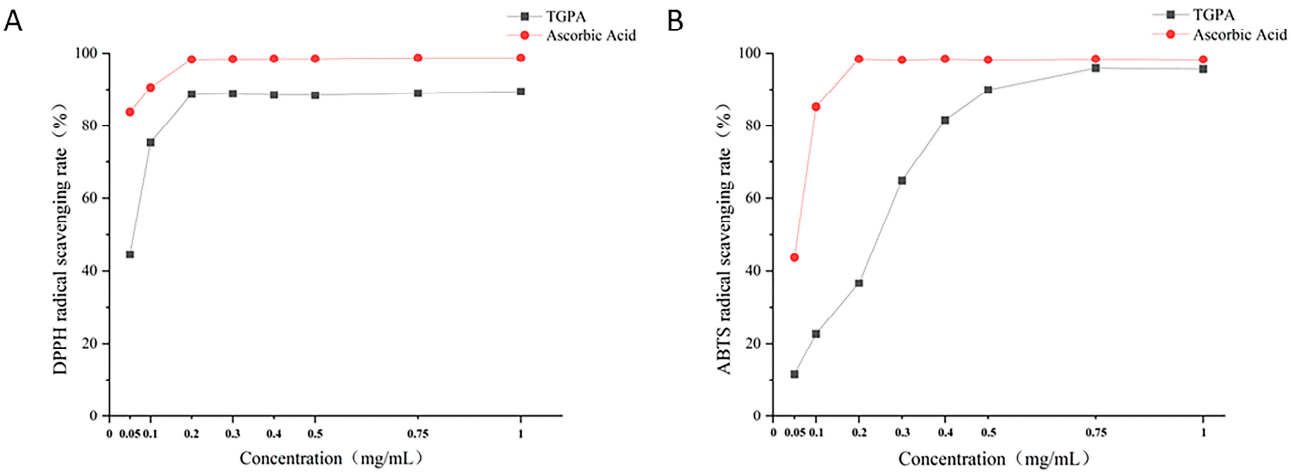


Figure 3. Effects of TGPA on scavenging DPPH (**A**) and scavenging ABTS (**B**).

3.3. Anti-Aging Activity

3.3.1. Effect of TGPA Extract on the Lifespan of *Caenorhabditis elegans*

Nematodes were cultured under blank control conditions and in the presence of TGPA at 0.25 mg/mL, 0.5 mg/mL, and 0.75 mg/mL. The survival curves of the treated and control groups are shown in Figure 4.

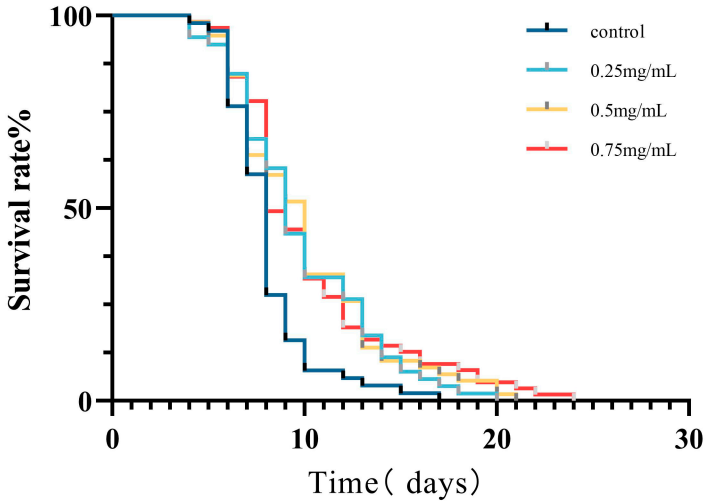


Figure 4. Survival curves of *Caenorhabditis elegans* treated with TGPA (0, 0.25, 0.5, and 0.75 mg/mL).

As shown in Table 4, the average lifespan of the blank control group was 8.06 ± 0.58 days. Nematodes treated with 0.25 mg/mL, 0.5 mg/mL, and 0.75 mg/mL TGPA demonstrated mean lifespans of 9.83 ± 0.34 days, 10.05 ± 0.42 days, and 10.16 ± 0.31 days, respectively, representing lifespan extensions of 21.83%, 24.68%, and 26.05% relative to the control. Significant lifespan extension ($p < 0.05$) occurred in the 0.5 mg/mL and 0.75 mg/mL groups, whereas the 0.25 mg/mL group showed no statistically significant increase. These results demonstrate that TGPA effectively delays natural aging in *Caenorhabditis elegans*, with the protective effect increasing with concentration over the tested range. From a molecular perspective, lifespan extension may be associated with the regulation of aging-related signaling pathways by TGPA. Previous studies have demonstrated that the lifespan of Caenorhabditis elegans is modulated by pathways such as the insulin/insulin-like growth factor signaling (IIS) cascade, FOXO transcription factors, and SKN-1 [29,30].

Table 4. Statistical table indicating the survival time of *Caenorhabditis elegans* treated with TGPA (0, 0.25, 0.5, and 0.75 mg/mL).

Group	Maximum Lifespan (Days)	Average Lifespan (Days)	*p*
Control	17	8.06 ± 0.58	——
0.25	20	9.83 ± 0.34	>0.05
0.5	21	10.05 ± 0.42 *	<0.05
0.75	25	10.16 ± 0.31 *	<0.05

Note: * indicates significant difference, $p < 0.05$.

3.3.2. Effect of TGPA on Locomotor Ability in *Caenorhabditis elegans*

Muscle function in nematodes declines with aging, making locomotor ability a sensitive indicator of physiological aging [31]. As shown in Figure 5, the proportion of spontaneously motile Class A nematodes decreased progressively across all groups with increasing age. By day 6, the percentage of Class A nematodes in the blank control group was consistently lower than that in all TGPA-treated groups, indicating an earlier onset of motor decline in untreated worms. The percentages of Class B and Class C nematodes were also lower in the TGPA-treated groups than in the control group, suggesting that supplementation with TGPA helped preserve neuromuscular function. By day 9, the locomotor ability of TGPA-treated nematodes remained significantly higher than that of the blank control group. The proportion of Class C nematodes in the blank group reached 20.00%, compared with 16.67%, 11.67%, and 10.00% in the TGPA-treated groups, respectively. The underlying response mechanisms may involve TGPA-mediated protection of neuromuscular function. During aging, the muscle cells of Caenorhabditis elegans undergo oxidative damage, which leads to structural abnormalities in contractile proteins such as actin and myosin. The antioxidant activity of TGPA can mitigate the accumulation of reactive oxygen species (ROS), thereby protecting muscle cells from oxidative stress and preserving locomotor function. These findings indicate that TGPA significantly improves locomotor activity in aging nematodes and delays their functional decline.

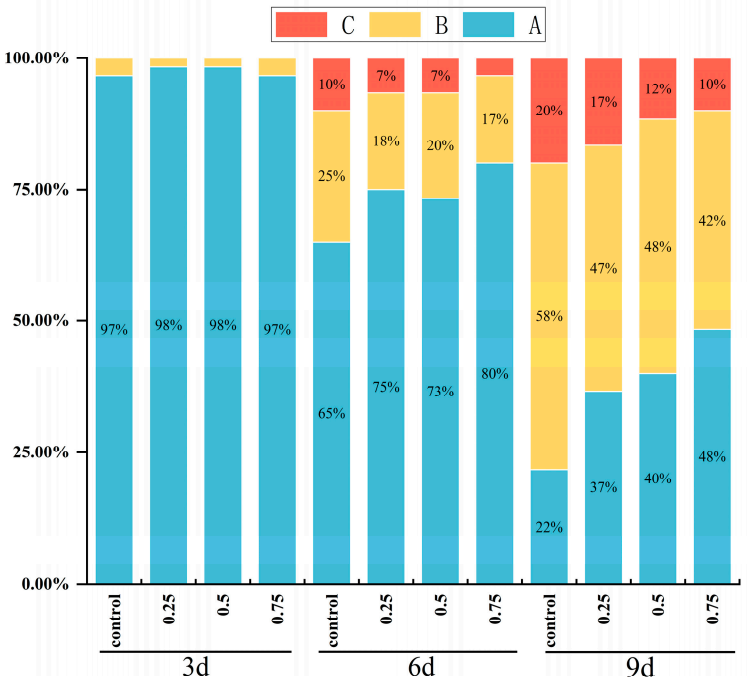


Figure 5. Effects of TGPA on the Motility of *Caenorhabditis elegans*.

3.3.3. Effect of TGPA on Nematode Fertility

Fertility in *Caenorhabditis elegans*, as reflected in egg production, closely correlates with aging and is therefore a key indicator of physiological decline [32]. As shown in Figure 6A, egg production peaked on day 2 across all groups and was significantly higher on this day than on other days. The control group exhibited the highest egg production on day 2, followed by a more rapid decline in subsequent days, indicating an earlier onset of reproductive aging. TGPA treatment moderately extended the duration of reproductive activity, with treated nematodes maintaining egg-laying ability for a longer period compared with controls. As shown in Figure 6B, no significant differences in total egg production were observed among the groups. These findings suggest that TGPA extends lifespan in *Caenorhabditis elegans* without compromising reproductive capacity, further supporting its anti-aging effects.

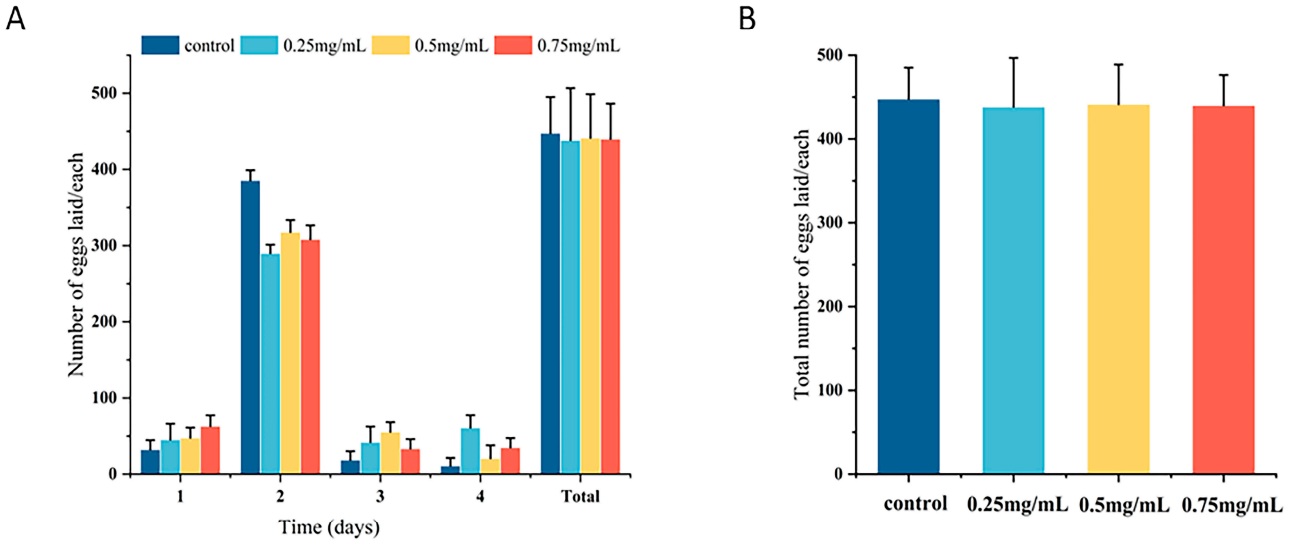


Figure 6. Effects of TGPA on the Reproductive Capacity of *Caenorhabditis elegans* (**A**,**B**).

3.3.4. Effects of TGPA on Heat Stress in Nematodes

The lifespan of *Caenorhabditis elegans* is closely associated with its tolerance to external stressors. Heat resistance under high-temperature exposure is a widely used indicator of anti-aging capacity, as improved heat tolerance generally correlates with increased stress resistance [33]. As shown in Figure 7, nematodes treated with 1 mg/mL, 2 mg/mL, and 3 mg/mL TGPA exhibited improved heat stress resistance, with mean lifespan increases of 5.96%, 13.17%, and 24.14%, respectively, compared with the control group. The 3 mg/mL TGPA treatment achieved the longest survival time under heat stress, reaching 10 h. Lifespan extension in all TGPA-treated groups was significantly higher than that of the control group ($p < 0.05$). These results indicate that TGPA increases nematode resistance to heat-induced physiological damage, demonstrating a clear protective effect against heat stress.

3.3.5. Effects of TGPA Extract on Acute Oxidative Stress Damage Induced by Hydrogen Peroxide in Nematodes

The protective effects of TGPA on oxidative stress–induced injury in *Caenorhabditis elegans* are shown in Figure 7. Following TGPA treatment, nematodes exhibited significantly increased tolerance to hydrogen peroxide–induced oxidative stress. The average lifespan of the blank control group was 186.5 ± 6.3 min. On the other hand, nematodes treated with 2 mg/mL and 3 mg/mL TGPA achieved average lifespans of 191.0 ± 7.8 min and 201.0 ± 7.3 min, respectively, representing increases of 7.77% and 17.69% relative to controls ($p < 0.05$). Regarding maximum lifespan, nematodes in the 3 mg/mL group reached a

maximum survival of 330 min, whereas the control group reached 270 min. The 1 mg/mL and 2 mg/mL groups reached maximum lifespans of 300 min. These results demonstrate that TGPA significantly increases oxidative stress resistance in *Caenorhabditis elegans*, with a dose-dependent trend indicating higher protection at higher TGPA concentrations.

From a physiological perspective, under heat stress, TGPA may activate the HSF-1 signaling pathway to promote the expression of heat shock proteins (such as hsp-70), thereby repairing heat-damaged proteins [34–36]. Under oxidative stress, TGPA enhances the activity of antioxidant enzymes, such as SOD and CAT, reducing the accumulation of ROS and MDA [37–39]. Moreover, TGPA may regulate mitochondrial function, improve energy metabolism, and enhance the stress adaptation capacity of Caenorhabditis elegans [39]

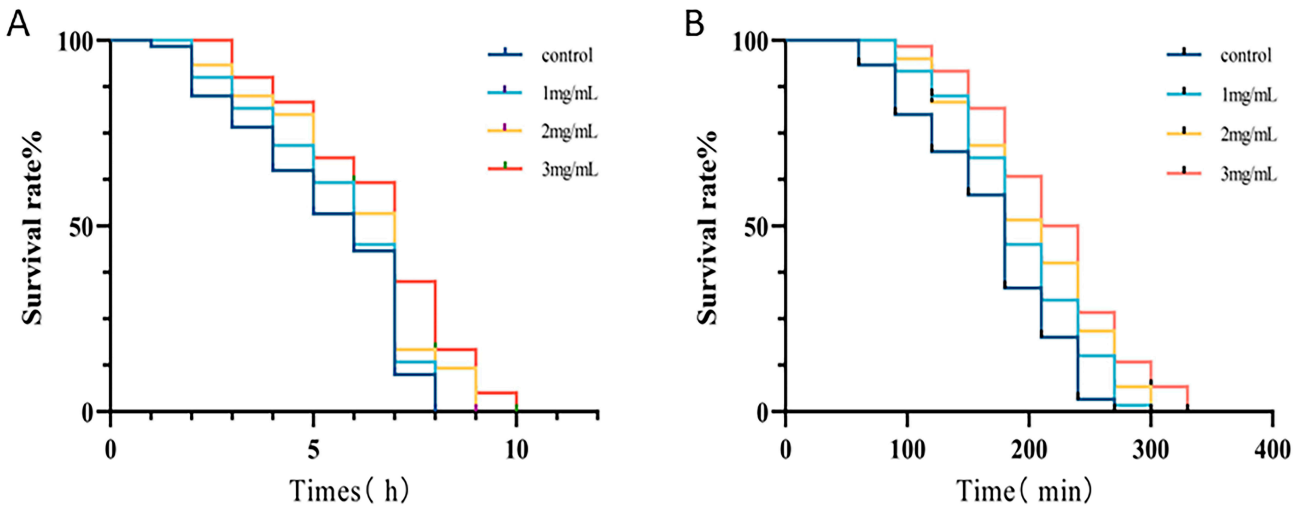


Figure 7. Survival curves of *Caenorhabditis elegans* treated with ABTS (0, 1, 2, and 3 mg/mL) following heat stress (37 °C) (**A**) and hydrogen peroxide stimulation (**B**).

4. Discussion

From a molecular pathway perspective, TGPA may exert its effects through multiple mechanisms: first, by activating the FOXO/daf-16 pathway, it upregulates the expression of antioxidant genes such as sod-3 and ctl-1, enhancing the activity of antioxidant enzymes [40]; second, by modulating the SKN-1 pathway, it promotes the expression of detoxification genes like gst-4, reducing ROS accumulation [41–43]; third, by influencing the HSF-1 signaling pathway, it increases the expression of heat shock proteins, thereby enhancing protein homeostasis [44]. Furthermore, TGPA does not affect the reproductive ability of Caenorhabditis elegans, which is an advantage over certain other anti-aging substances (e.g., some polysaccharides mildly suppress reproduction). This highlights its "healthy aging" benefits, possibly due to TGPA's precise regulation of aging pathways without interfering with the expression of reproductive-related genes.

Beyond pathway activation, structure–activity relationships (SAR) appear critical for the efficacy and specificity of these bioactive compounds. Anthocyanins differ markedly in their glycosylation patterns, aglycone cores, and degree of polymerization, all of which influence cellular uptake, stability, and interaction with molecular targets. For example, fermentation of purple sweet potato anthocyanins into smaller phenolic acids increased bioavailability and upregulated longevity-associated genes including daf-16, hsp-16.2, and skn-1 more effectively than their native forms, indicating that metabolic transformation and compound structure significantly affect biological outcomes [45]. Similarly, the abundance of petunidin-3-O-glucoside in black goji anthocyanins was closely associated with improved stress resistance and lifespan extension, suggesting that specific substituents enhance engagement with key signaling proteins [46].

Comparative evidence also highlights potential limitations of polyphenol interventions. Grape pomace extracts enriched in polyphenols increased stress resistance in *C. elegans* and extended maximum lifespan at certain moderate concentrations, but higher doses were detrimental, indicating hormetic dose responses that may depend on compound composition and structural complexity [47]. This contrasts with TGPA's consistent benefits in our assays, suggesting that extraction optimization and anthocyanin profile may confer advantages in both potency and safety.

This study is the first to systematically optimize the extraction process of anthocyanins from Tannat grape pomace, filling a gap in the resource utilization of by-products from this grape variety. It complements existing research on the pomace substances of other grape varieties. Meanwhile, the antioxidant and anti-aging activities of TGPA are superior to those of several reported natural products, offering a new option for the development of efficient antioxidant and anti-aging functional ingredients. Moreover, TGPA exerts its anti-aging effects without compromising reproductive ability, enhancing the safety and practical value of its application. Additionally, by converting agricultural waste into high-value natural compounds, this work contributes to resource recycling, reduces environmental burdens, and offers a low-cost raw material source for the natural active ingredient and functional food industries. Such utilization aligns with the principles of the green circular economy and supports the sustainable expansion of value chains in viticulture and agriculture.

However, several limitations should be acknowledged. First, in vitro antioxidant assays do not account for dynamic metabolic, absorption, and biotransformation processes that occur in vivo. Second, we did not purify the crude extract to identify the specific bioactive constituents responsible for the observed effects, nor did we delineate the precise molecular pathways through which these effects are mediated. Third, while *Caenorhabditis elegans* provides a convenient and highly informative model, its biological complexity is limited, restricting the ability to directly extrapolate findings to mammals. These limitations narrow the translational scope of the present results.

Future research should therefore extend this work to in vivo animal studies, purify and characterize the active constituents within the crude extract, and elucidate the precise molecular pathways using advanced multi-omics and mechanistic approaches, ultimately progressing toward evaluation in mammalian models and preliminary clinical investigations.

5. Conclusions

This study used RSM based on a Box–Behnken design to optimize the extraction of total anthocyanin glycosides (TGPA) from Tannat wine grape pomace. The optimal extraction parameters were identified as an extraction temperature of 51.27 °C, an ethanol concentration of 53.46%, an ultrasonication time of 20.10 min, and a solid-to-liquid ratio of 1:24.05, yielding a TGPA content of 189.21 ± 1.03 mg/100 g. The crude extract exhibited strong in vitro antioxidant activity, with clear concentration-dependent increases in DPPH and ABTS radical scavenging abilities. At 0.2 mg/mL, TGPA achieved a DPPH scavenging rate of 89.44% ± 0.87% (IC_{50} = 0.09 mg/mL), while 0.75 mg/mL resulted in an ABTS scavenging rate of 95.83% ± 0.54% (IC_{50} = 0.26 mg/mL). The *Caenorhabditis elegans* assays further demonstrated the biological efficacy of TGPA. Concentrations of 0.5 mg/mL and 0.75 mg/mL significantly prolonged lifespan and improved locomotor performance ($p < 0.05$). At higher concentrations (3 mg/mL), TGPA increased resistance to heat and oxidative stress without compromising reproductive output, underscoring its anti-aging potential.

These findings confirm that TGPA from grape pomace possesses significant antioxidant and geroprotective properties. This study represents a pioneering effort to de-

velop anthocyanin-based functional ingredients from Tannat grape pomace, a winemaking byproduct.

Author Contributions: Conceptualization, B.W.; methodology, B.W. and H.W.; software, B.W.; validation, B.W., Y.Y. and H.W.; formal analysis, B.W. and Y.Y.; investigation, B.W. and Y.Y.; resources, B.W., Y.Y. and H.W.; data curation, B.W.; writing—original draft preparation, B.W.; writing—review and editing, B.W. and H.W.; visualization, B.W.; supervision, H.W.; project administration, B.W. and Y.Y.; funding acquisition, H.W. All authors have read and agreed to the published version of the manuscript.

Funding: This research was funded by Project on Establishing a Practical Teaching System for Cultivating High-Level Talent in Modern Agriculture under the New Agricultural Sciences Paradigm, Yantai Municipal Education Bureau 2022 campus integration project and 2022 Yantai University-Community Integration Funding Project. The APC was funded by Yantai Institute of China Agricultural University.

Institutional Review Board Statement: Not applicable.

Data Availability Statement: The data that support the findings of this study are available from the corresponding author upon reasonable request.

Acknowledgments: This work was supported by the Microbiology and Food Science Laboratory of China Agricultural University. Weifu Kong provided financial support and valuable guidance throughout the study. Meanwhile, thanks to other teachers, lab mates, and my family for their support. I also appreciate Yantai Municipal Education Bureau's financial aid and the journal reviewers' valuable comments.

Conflicts of Interest: The authors declare no conflicts of interest. The funding agency did not participate in any part of the research process.

Abbreviations

The following abbreviations are used in this manuscript:

TGPA	Tannat Grape Pomace Anthocyanins
DPPH	2,2-Diphenyl-1-picrylhydrazyl
ABTS	2,2′-Azino-bis(3-ethylbenzothiazoline-6-sulfonic acid)
RSM	Response surface methodology

References

1. Largado-Valler, D. In-Vitro Production of Anthocyanin in Sesbania grandiflora (Red Katuray) as Influenced by Varying Concentrations of 2,4-D and BA Added on MS Medium. *Am. J. Plant Sci.* **2016**, *7*, 2297–2306. [CrossRef]
2. Ayuda-Durán, B.; González-Manzano, S.; Gil-Sánchez, I.; Moreno-Arribas, M.V.; Bartolomé, B.; Sanz-Buenhombre, M.; Guadarrama, A.; Santos-Buelga, C.; González-Paramás, A.M. Antioxidant Characterization and Biological Effects of Grape Pomace Extracts Supplementation in *Caenorhabditis elegans*. *Foods* **2019**, *8*, 75. [CrossRef] [PubMed]
3. Cai, J.Q.; Qin, X.M.; Lu, H.Y.; Ye, W.Q.; Zhang, G.F.; Lin, H.S.; Zheng, H.N. Anti-aging effect of Abalone muscle enzymatic hydrolysate on *Caenorhabditis elegans*. *Food Ferment. Ind.* **2023**, *49*, 106–112.
4. Chen, H. Study on Functional Food and Biological Activity of *Aronia melanocarpa* Fruit. Master's Thesis, Jilin University of Chemical Technology, Jilin, China, June 2024.
5. Chen, X.; Lu, S.; Zou, Z.; Chen, J.; Huang, L.; Li, P.; Du, B. The Anti-Aging Effect of Tianlu Black-Bone Chicken Soup on *Caenorhabditis elegans*. *Food Ferment. Ind.* **2025**, 1–12. [CrossRef]
6. Cuiping, Y.I.; Sijie, Z.; Jinxiang, X.; Bo, Z.; Li, Z. Antioxidant activity of rice bran fermentation broth and its effect on the longevity of *Caenorhabditis elegans*. *Food Ferment. Ind.* **2025**, 70–75. [CrossRef]
7. Dehghan, E.; Zhang, Y.; Saremi, B.; Yadavali, S.; Hakimi, A.; Dehghani, M.; Goodarzi, M.; Tu, X.; Robertson, S.; Lin, R.; et al. Hydralazine induces stress resistance and extends *C. elegans* lifespan by activating the NRF2/SKN-1 signalling pathway. *Nat. Commun.* **2017**, *8*, 2223. [CrossRef]
8. Gerardi, C.; D'amico, L.; Migoni, D.; Santino, A.; Salomone, A.; Carluccio, M.A.; Giovinazzo, G. Strategies for Reuse of Skins Separated from Grape Pomace as Ingredient of Functional Beverages. *Front. Bioeng. Biotechnol.* **2020**, *8*, 645. [CrossRef]

9. Granese, T.; Cardinale, F.; Cozzolino, A.; Pepe, S.; Ombra, M.N.; Nazzaro, F.; Coppola, R.; Fratianni, F. Variation of Polyphenols, Anthocyanins and Antioxidant Power in the Strawberry Grape (*Vitis labrusca*) after Simulated Gastro-Intestinal Transit and Evaluation of in Vitro Antimicrobial Activity. *Food Nutr. Sci.* **2014**, *5*, 60–65. [CrossRef]
10. Hou, Z.; Zhu, D.; Gao, X.; Zhao, L.; Yang, H.; Wang, Q.; Zhao, Y.; Wang, N. Antiaging and antioxidative effects of water extract of *Zizyphus jujuba* Mill on *Caenorhabditis elegans*. *J. Funct. Foods* **2023**, *110*, 105829. [CrossRef]
11. Huang, J.; Liu, Z.-G.; Mu, L.-Q.; Fu, Y.-J. Research Progress on Extraction and Purification of Anthocyanins. *Chem. Reag.* **2021**, 1683–1690.
12. Huang, S.; Chen, H.; Zhong, C.; Zhu, S.; Li, P.; Du, B. Anti-aging Effect of Polysaccharide from *Dendrobium officinale* Leaves in *Caenorhabditis elegans*. *Food Sci.* **2022**, *43*, 203–208. [CrossRef]
13. Jolly, E.; Goupy, P.; Claisse-Gainvors, A.; Dangles, O.; Garcia-Bernet, D.; Dufour, C.; Rémond, C. A two-step biocatalytic process to extract and to acylate anthocyanins: A sustainable approach for red grape pomace biorefining. *Appl. Food Res.* **2025**, *5*, 101431. [CrossRef]
14. Wang, J. Multidimensional Omics Analysis to Explore the Anti-Aging Mechanism of *Anoectochilus roxburghii* Extract in *Caenorhabditis elegans*. Master's Thesis, Zhejiang Normal University, Jinhua, China, 2024.
15. Kovács, D.; Biró, J.B.; Ahmed, S.; Kovács, M.; Sigmond, T.; Hotzi, B.; Varga, M.; Vincze, V.V.; Mohammad, U.; Vellai, T.; et al. Age-dependent heat shock hormesis to HSF-1 deficiency suggests a compensatory mechanism mediated by the unfolded protein response and innate immunity in young *Caenorhabditis elegans*. *Aging Cell* **2024**, *23*, e14246. [CrossRef]
16. Kumsta, C.; Hansen, M. Hormetic heat shock and HSF-1 overexpression improve *C. elegans* survival and proteostasis by inducing autophagy. *Autophagy* **2017**, *13*, 1076–1077. [CrossRef] [PubMed]
17. Lei, W.; Jiayi, Q.; Zhijin, Z.; Tianyi, C.; Yingxing, X.; Xuzheng, C.; Caisheng, W.; Guoying, Q. Effects of *Laminaria japonica* Oligosaccharides on Antioxidant Enzyme Activities and Anti-Aging in *Drosophila melanogaster*. *Sci. Technol. Food Ind.* **2025**, 1–16. [CrossRef]
18. Li, D.; Wang, P.; Luo, Y.; Zhao, M.; Chen, F. Health benefits of anthocyanins and molecular mechanisms: Update from recent decade. *Crit. Rev. Food Sci. Nutr.* **2017**, *57*, 1729–1741. [CrossRef] [PubMed]
19. Li, L.D.; Wang, S.Y.; Li, X.Y.; Wang, Q.; Chen, T.; Yu, X.; Xiao, M.; Ma, T.P.; Xie, Y.Q. The Anti-Aging Effects of Shuquan Yishen Formula in *C. elegans* Through Antimetabolic Dysregulation and Antioxidant Stress. *Chin. Tradit. Pat. Med.* **2025**, *47*, 1642–1646. [CrossRef]
20. Li, M.-S. Study on the Effects of Anthocyanin of Aronia on Human Gastric Cancer Cell SGC-7901. *Territ. Nat. Resour. Study* **2016**, 90–92. [CrossRef]
21. Li, Z.; Hao, H.; Jiang, H.; Jia, Z.; Caifen, L. Research Status and Prospects of the Antioxidant Activity of Anthocyanins. *Food Ind.* **2019**, 238–243.
22. Lin, C.; Zhang, X.; Xiao, J.; Zhong, Q.; Kuang, Y.; Cao, Y.; Chen, Y. Effects on longevity extension and mechanism of action of carnosic acid in *Caenorhabditis elegans*. *Food Funct.* **2019**, *10*, 1398–1410. [CrossRef]
23. Liu, Y.; Wu, J.; Ding, Z.; Chen, L.; Liu, M.; Li, B.; Li, X.; Li, J.; Liu, W. Verbascoside from *Callicarpa nudiflora* Hook extends lifespan in *Caenorhabditis elegans* via SKN-1 pathway activation. *Biogerontology* **2025**, *27*, 18. [CrossRef]
24. Luan, Y.; Jiang, Y.; Huang, R.; Wang, X.; He, X.; Liu, Y.; Tan, P. Polygonati Rhizoma Polysaccharide Prolongs Lifespan and Healthspan in *Caenorhabditis elegans*. *Molecules* **2023**, *28*, 2235. [CrossRef] [PubMed]
25. Najiao, Z.; Li, Y.; Longmei, G.; Mingyang, W.U. Advances in Research on Extraction Process and Analytical Method of Anthocyanin in Purple Potatoes. *Process Technol.* **2025**, 102–105. [CrossRef]
26. Lyu, Q.J.; Gan, Z.S.; Che, G.Z.; Rao, J.W. Research Progress on the Bioactive of Anthocyanins in Black Rice. *China Food Saf. Mag.* **2024**, 94–96.
27. Sadowska-Bartosz, I.; Bartosz, G. Antioxidant Activity of Anthocyanins and Anthocyanidins: A Critical Review. *Int. J. Mol. Sci.* **2024**, *25*, 12001. [CrossRef]
28. Song, B.; Zheng, B.; Li, T.; Liu, R.H. Raspberry extract ameliorates oxidative stress in *Caenorhabditis elegans* via the SKN-1/Nrf2 pathway. *J. Funct. Foods* **2020**, *70*, 103977. [CrossRef]
29. Song, Z.; Huang, Y.; Wang, Y.; Deng, J.; Zhen, D.; Tan, N.; Cheng, S. Antioxidant and anti-aging effects and mechanism of *Poria cocos polysaccharides* in *Caenorhabditis elegans*. *Chin. Tradit. Herb. Drugs* **2024**, *55*, 1133–1144.
30. Su, Y.; Jiang, Y.; Xiaobin, D.; Buyang, C. The Impact of col-93 on Locomotion and Aging in *Caenorhabditis elegans* Through Regulation of the Heat Shock Factor-1 Signaling Pathway. *Chin. J. Cell Biol.* **2025**, *47*, 3088–3098. [CrossRef]
31. Sugawara, T.; Sakamoto, K. Quercetin enhances motility in aged and heat-stressed *Caenorhabditis elegans* nematodes by modulating both HSF-1 activity, and insulin-like and p38-MAPK signalling. *PLoS ONE* **2020**, *15*, e0238528. [CrossRef]
32. Turrini, E.; Ferruzzi, L.; Fimognari, C. Possible Effects of Dietary Anthocyanins on Diabetes and Insulin Resistance. *Curr. Drug Targets* **2017**, *18*, 629–640. [CrossRef] [PubMed]
33. Wang, T. Study on the Anti-Aging Effect and Mechanisms of Berberine in *Caenorhabditis elegans*. Master's Thesis, Jilin University, Changchun, China, 2025.

34. Wang, W.; Li, S.; Zhu, Y.; Zhu, R.; Du, X.; Cui, X.; Wang, H.; Cheng, Z. Effect of Different Edible *Trichosanthes germplasm* on Its Seed Oil to Enhance Antioxidant and Anti-Aging Activity in *Caenorhabditis elegans*. *Foods* **2024**, *13*, 503. [CrossRef] [PubMed]
35. Wei, R.X.; Lu, H.Y.; Qin, X.M.; Wang, L.Y. Study on the Anti-Aging Effects of Oyster Extract on *Caenorhabditis elegans*. *Food Ferment. Ind.* **2024**, *50*, 52–58. [CrossRef]
36. Xiang, Y.; Lai, F.; He, G.; Li, Y.; Yang, L.; Shen, W.; Huo, H.; Zhu, J.; Dai, H.; Zhang, Y. Alleviation of Rosup-induced oxidative stress in porcine granulosa cells by anthocyanins from red-fleshed apples. *PLoS ONE* **2017**, *12*, e0184033. [CrossRef] [PubMed]
37. Xin, M.; Liang, Q.; Tian, J.; Yang, S.; Yang, Y.; Li, B. Effects of Sucrose Degradation Products on the Stability and Antioxidant Activity of Blueberry Anthocyanins Under Processing and Storage Conditions. *Shipin Kexue/Food Sci.* **2024**, *45*, 51–59. [CrossRef]
38. Xu, Q.; Zheng, B.; Li, T.; Liu, R.H. Black goji berry anthocyanins extend lifespan and enhance the antioxidant defenses in *Caenorhabditis elegans* via the JNK-1 and DAF-16/FOXO pathways. *J. Sci. Food Agric.* **2025**, *105*, 2282–2293. [CrossRef]
39. Tang, X.B.; Zhang, C.; Wang, L.Y.; Liang, S.Y.; Ou, L.L. Optimization of the Extraction Process of Total Saponins from Asparagus Cochinchinensis Peel and Study on its Anti-Aging Effects on *Caenorhabditis elegans*. *Chin. Pharm. J.* **2025**, 2293–2302.
40. Yu, M.; Wang, B.; Xu, H.; Li, Q.; Wu, J.; Shang, X. Research Progress on the Reuse of Grape Skin Residue. *Shandong Chem. Ind.* **2021**, *50*, 84–87. [CrossRef]
41. Zhang, S.; Lyu, X.; Liu, W.; Zhang, J. Research progress on physical and chemical characteristics, extraction technology, and functional activity of anthocyanins from fruits and vegetables. *Food Ferment. Ind.* **2024**, *50*, 360–371. [CrossRef]
42. Zhang, X.; Chen, Q.; Chen, L.; Chen, X.; Ma, Z. Anti-Aging in *Caenorhabditis elegans* of Polysaccharides from *Polygonatum cyrtonema* Hua. *Molecules* **2024**, *29*, 1276. [CrossRef]
43. Zhao, D.; Yan, M.; Xu, H.; Liang, H.; Zhang, J.; Li, M.; Wang, C. Antioxidant and Antiaging Activity of Fermented Coix Seed Polysaccharides on *Caenorhabditis elegans*. *Nutrients* **2023**, *15*, 2474. [CrossRef]
44. Zhao, J.; Yu, J.; Zhi, Q.; Yuan, T.; Lei, X.; Zeng, K.; Ming, J. Anti-aging effects of the fermented anthocyanin extracts of purple sweet potato on *Caenorhabditis elegans*. *Food Funct.* **2021**, *12*, 12647–12658. [CrossRef] [PubMed]
45. Zhou, M.; Wu, C.; Xu, W.; Liu, T.; Zhang, S.; Yan, H.; Yang, Z. Optimization in Extraction Strategy of Anthocyanins from Blueberry Pomace Based on Plackett-Burman Design and Response Surface Methoddogy. *Food Sci. Technol.* **2024**, *50*, 231–239. [CrossRef]
46. Chen, Z.W.; Ren, Y.M.; Tang, X.; Nie, S.M.; Ma, D.W. Mechanism of *Gymnadenia orchidis* Alcohol Extract in Delaying Aging in *Caenorhabditis elegans* via the Antioxidant Pathway. *Food Sci.* **2025**.
47. Zhu, A.; Zheng, F.; Zhang, W.; Li, L.; Li, Y.; Hu, H.; Wu, Y.; Bao, W.; Li, G.; Wang, Q.; et al. Oxidation and Antioxidation of Natural Products in the Model Organism *Caenorhabditis elegans*. *Antioxidants* **2022**, *11*, 705. [CrossRef]

Disclaimer/Publisher's Note: The statements, opinions and data contained in all publications are solely those of the individual author(s) and contributor(s) and not of MDPI and/or the editor(s). MDPI and/or the editor(s) disclaim responsibility for any injury to people or property resulting from any ideas, methods, instructions or products referred to in the content.